Resonant Spin Amplification in *n*-Type GaAs

J. M. Kikkawa and D. D. Awschalom

Department of Physics, University of California, Santa Barbara, California 93106
(Received 11 December 1997)

Extended electron spin precession in *n*-type GaAs bulk semiconductors is directly observed by femtosecond time-resolved Faraday rotation in the Voigt geometry. Synchronous optical pumping of the spin system amplifies and sustains spin motion, exposing a regime where spin lifetimes increase tenfold at low fields and exceed 100 ns at zero field. Precise studies in field and temperature provide clues to the relevant electron relaxation mechanisms, indicating a strong dependence on doping concentration. [S0031-9007(98)06021-9]

An emerging interest within the physics community is the use of electronic spins within semiconductors for the storage of coherence [1] and as a medium for a variety of integrated magnetoelectronic applications involving polarized transport [2]. For both, it is desirable to know the limitations imposed by environmental spin decoherence and to understand how these may be influenced by temperature and ambient magnetic fields. Through all-optical studies of spin precession using time-resolved Faraday rotation (TRFR), we recently showed that a two-dimensional electron gas can act as a reservoir for optically injected spin polarization, significantly extending spin lifetimes by removing holes which act to efficiently scatter electron spins [3]. While studies of moderately *n*-doped bulk II-VI semiconductors showed similar behavior [3], here we find in bulk GaAs that lowering the doping level (and thus the electron kinetic energy) uncovers a completely different regime in which spin lifetimes become strongly field and temperature dependent and are further extended 2 orders of magnitude at low temperature. To explore these new dynamics, we introduce a method of resonant spin amplification, in which the synchronous injection of electron spins in phase with their precession yields a tenfold increase in spin polarization and a series of sharp field-dependent resonances. These resonances are sensitive probes of spin scattering and dephasing, and reveal a power-law divergence of the spin lifetime as the applied field is lowered towards zero.

Si-doped GaAs single crystals are prepared with room-temperature doping densities $n = 1 \times 10^{16}$, 1×10^{18}, and 5×10^{18} cm^{-3} and mobilities $\mu = 5400$, 2300, and 1340 cm^2/V s, respectively. A semi-insulating GaAs sample was studied as a control, heretofore referred to as $n \approx 0$. All wafers are thinned to ~ 50 μm by mechanical polishing and mounted strain-free in a magneto-optical cryostat. A Hall sensor on the sample support records the applied magnetic field to a resolution of better than 10^{-5} T. A mode-locked Ti:sapphire laser provides 100 fs pump and probe pulses whose relative delay is adjusted by a conventional delay line. For synchronous pumping experiments, the laser repetition interval t_{rep} is fixed at 13.157 ± 0.0015 ns by actively stabilizing the cavity length.

Here TRFR in the Voigt geometry measures the Larmor precession of electron spins excited by a normally incident, circularly polarized pump pulse [3]. Whereas holes spin-relax rapidly due to valence band mixing [4], a net electron spin rotates the probe's linear polarization, measured by a polarization bridge technique described elsewhere [3,5]. This deflection is proportional to the electron moment along the probe's normal incidence, so spin precession about an in-plane magnetic field B causes the Faraday rotation to oscillate in the pump-probe delay, Δt. Scanning Δt then produces a TRFR profile of the form $A e^{-\Delta t/T_2^*} \cos(g \mu_B H \Delta t/\hbar)$, whose frequency is a direct measure of the electron *g* factor and whose decay yields the transverse spin lifetime, T_2^* [5].

This oscillatory temporal evolution is shown in Fig. 1 for the different doping concentrations at $T = 5$ K and
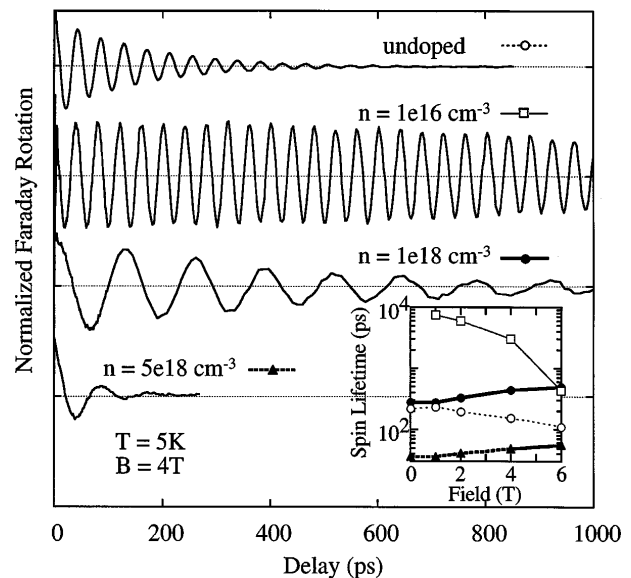

FIG. 1. TRFR for undoped and *n*-type GaAs at $B = 4$ T. Data are normalized just after zero pump-probe delay. Plots are offset for clarity, with zeros marked by dotted lines. The inset shows T_2^* vs field. Data are taken at $T = 5$ K with $N_{\text{ex}} = 2 \times 10^{14}$, 2×10^{14}, 1.4×10^{15}, and 3×10^{15} cm^{-3} for $n = 0$, 10^{16}, 10^{18}, and 5×10^{18}, respectively.

$B = 4$ T. Doping within this regime leads to shifts in the absorption edge [6], and low energy carriers are excited by a laser spectrum (FWHM = 7 meV) centered at an energy of 1.514, 1.531, and 1.556 eV for $n = 1 \times 10^{16}$, 1×10^{18}, and 5×10^{18}, respectively. A change in Larmor frequency with doping reflects an energy dispersion in the GaAs conduction band g factor [7]. Because we observe that increased excitation densities N_{ex} degrade T_2^* in nondegenerate samples, N_{ex} is kept several orders of magnitude below n. For $n \approx 0$, the laser energy (1.540 eV) includes an additional 20 meV which does not significantly affect the free electron spin lifetime and suppresses the excitation of excitons whose precession complicates data analysis. The free carrier spin lifetime is a nonmonotonic function of carrier density, abruptly increasing between the $n \approx 0$ and $n = 1 \times 10^{16}$ samples and steadily decreasing thereafter. The inset shows T_2^* vs field, spanning over 2 orders of magnitude and ranging from nearly 10 ns for $n = 1 \times 10^{16}$ to less than 40 ps for $n = 5 \times 10^{18}$. For $n = 1 \times 10^{16}$, the zero-field polarization exhibits virtually no decay in the 1 ns measurement interval, making its lifetime difficult to quantify. Below, a technique which effectively extends the measurement interval shows that the range in lifetimes is over 3 orders of magnitude.

Qualitatively, T_2^* increases with field for the two highest doses and decreases for the two lowest. To understand this behavior, we consider processes which introduce a broadening, $\langle \Delta\phi^2 \rangle / 2$, to the spin direction ϕ [8]. If the resulting distribution is Gaussian, the spin polarization decays according to $\exp(-\langle \Delta\phi^2 \rangle / 2)$, and $(T_2^*)^{-1}$ equals the broadening rate Γ. Contributions to Γ may arise from spin-orbit scattering during collisions with phonons or impurities [the Elliot-Yafet (EY) mechanism [9]] or from precession about anisotropic internal magnetic fields [the D'yakanov-Perel' (DP) mechanism [10]]. In the former case, $\Gamma \propto \Gamma_P$, where Γ_P is the momentum scattering rate. In the latter case, the broadening accumulates between collisions, so $\Gamma \propto \Gamma_P^{-1}$. The application of a field adiabatically scatters electron momentum at the cyclotron frequency ω_c and suppresses DP relaxation by randomizing the internal field axis between collisions when $\omega_c \sim \Gamma_P$ [11]. The data suggest a DP mechanism for the two highest doping levels. We note that electron-hole spin scattering, important in p-type GaAs, is not a favored mechanism in these n-type samples because the number of holes injected yields a spin relaxation which is too slow by several orders of magnitude and is independent of n [12].

An additional contribution to the spin relaxation rate may arise from a spread in electronic g factors, Δg, which results in an inhomogeneous dephasing of ϕ given by $\Delta\phi = \Delta g \mu_B B t / \hbar$ [13]. When Δg represents a Gaussian variance, the nonexponential decay that follows is characterized by an effective lifetime $T = \hbar\sqrt{2}/\Delta g \mu_B B$. Because we do not find a general inverse relationship between T_2^* and B for $n = 0$ or 10^{16}, this process can be neglected over most of the field range. Moreover, for $n = 10^{16}$, the

measured spin lifetimes at 6 T imply that $\Delta g < 0.005$, and using the dispersion $g = -0.44 + 6.3E(\mathrm{eV})$ [7], this implies that spin precession occurs within a carrier energy width that is far less than its initial distribution, as determined by the excitation spectrum.

By measuring the Faraday rotation at a fixed pump-probe delay and sweeping the magnetic field, we monitor oscillations which are periodic in B at a frequency proportional to both Δt and g. Changes in the oscillation envelope reflect a field dependence in either T_2^* or the amplitude A. Figure 2(a) shows a field scan at $\Delta t = 1$ ns for $n = 1 \times 10^{16}$. Because T_2^* is long in this sample (Fig. 1 inset), a decrease in the TRFR is observable only above 4.5 T. A closer look at the lower-field region, expanded in Fig. 2(b), reveals the appearance of a second period. A power spectrum of Fig. 2(a) over the interval from 1 to 2.5 T is shown in Fig. 2(c), where the field periodicity is expressed as a temporal interval for the Larmor precession, $h/g\mu_B \Delta B$. The data show the peak at 1 ns expected from the pump-probe delay, and an additional feature arising from the high-field frequency oscillations. The latter corresponds to the pump's repetition interval t_{rep} and arises from an increased polarization when spin precession
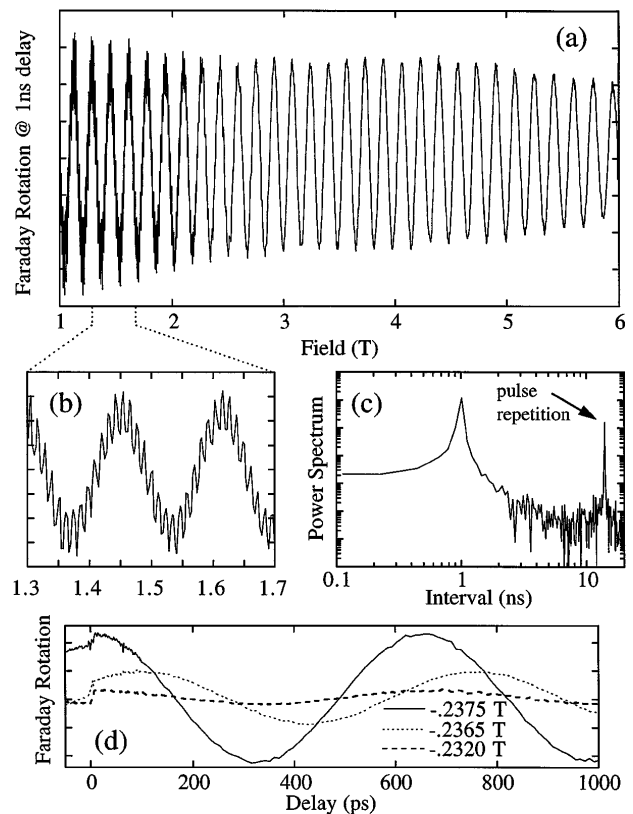

FIG. 2.   (a) TRFR for $n = 10^{16}$ taken at $\Delta t = 1$ ns. (b) An expanded view of (a). (c) The power spectrum of (a) taken over the interval from $B = 1$ to 2.5 T. The field periodicity is converted to a time interval, and the appearance of the laser repetition interval is indicated. (d) TRFR showing resonant and off-resonant behavior. Data for (a)–(d) are taken at $T = 5$ K with $N_{\mathrm{ex}} = 2 \times 10^{14}$ cm^{-3}.

is commensurate with the pulse repetition. By tuning the magnetic field so that the precession frequency is precisely resonant with the repetition interval, spin injection is always in phase with the precessing spin polarization. The result is an amplification that is fivefold at ~0.24 T [Fig. 2(d)] and more than tenfold at zero field. The phase of the total spin precession is visibly shifted relative to the pump by changing the field only 10 G (0.4%) off resonance, demonstrating the remarkable sensitivity of this effect. Moving the field another 35 G is sufficient to completely suppress the resonance and produces a small negative offset (visible when $\Delta t < 0$) arising from a net destructive interference of preceding pulses. These data imply that T_2^* is of the same order as t_{rep} at a field of ~1 T and increases with decreasing field, in agreement with Fig. 1 (inset).

Using this "resonant spin amplification," we obtain precise measurements of spin lifetimes well in excess of t_{rep}. Figures 3(a) and 3(b) show low-field studies of TRFR at fixed Δt. Dotted lines indicate zero Faraday rotation (theory fits are offset for clarity). While one ordinarily sees almost no field dependence at $\Delta t = 10$ ps,
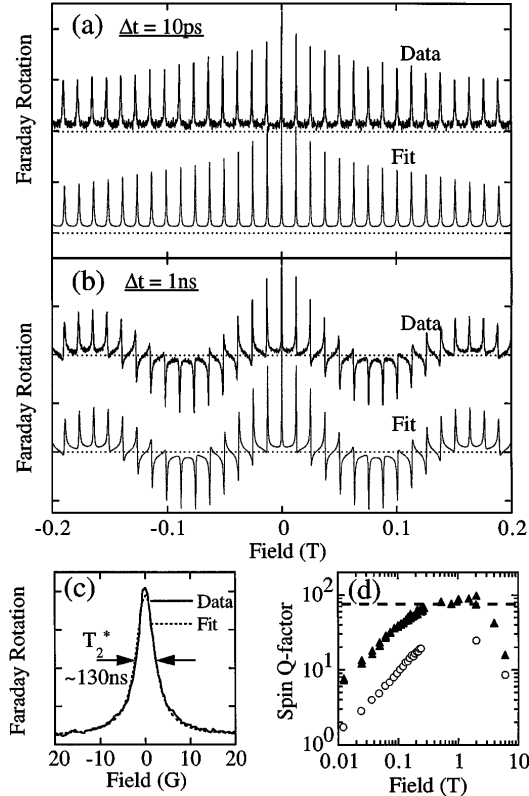

FIG. 3. TRFR for $n = 10^{16}$ at small magnetic fields with $\Delta t = 10$ ps (a), and 1 ns (b). Fits derive from Eq. (1) and are offset for clarity. Zeros are indicated by dotted lines. (c) An expanded view of the central resonance in (a). The fit given by the dotted line corresponds to a spin lifetime of 130 ns. (d) The spin Q factor vs field on a log-log plot. $N_{\text{ex}} = 2 \times 10^{14}$ cm^{-3} (solid triangles) and 3×10^{15} cm^{-3} (open circles), respectively. The dotted line indicates a thermal ceiling (described in the text). Data are taken at $T = 5$ K.

the data comprise a sequence of resonances, individually resolved in Fig. 3(c), which increase in amplitude and decrease in width as the field approaches zero. This behavior may be understood qualitatively as arising from increased spin lifetimes near $B = 0$, which require an increasing number of successive pump pulses to be in phase. Resonances are consequently narrower in field and concurrently amplified further because more spin polarization survives from each preceding spin excitation. At $\Delta t = 1$ ns, the resonances are seen to change sign because the spin resonance has precessed during the 1 ns interval before the probe's measurement. Their amplitude thus follows the slow oscillations which continue from Fig. 2(a), and resonances are joined by regions in which the phase shifts seen in Fig. 2(c) distort the oscillatory background. These notions are made quantitative by fitting the observed spin polarization M_s to the sum of exponentially decaying oscillations,

$$M_s(\Delta t, B) = \sum_n \Theta(\Delta t + nt_{\text{rep}}) A e^{-(\Delta t + nt_{\text{rep}})/T_2^*}$$
$$\times \cos[g\mu_B B(\Delta t + nt_{\text{rep}})/\hbar]. \quad (1)$$

Here n represents a sum over all laser pulses and the step function Θ ensures that only preceding pump pulses contribute to M_s at any particular delay Δt. Data are fit by adjusting T_2^*, A, and g separately for each resonance (except at zero field, where g is interpolated). The results are shown in Figs. 3(a) and 3(b), where excellent agreement for both delays (and over the *entire* interval from -10 ps to 1 ns) is obtained with identical fitting parameters. In this manner, T_2^* may be extracted for each resonance, and is seen to increase by tenfold from 1 to 0 T, reaching 130 ns at zero field [Fig. 3(c)].

Because t_{rep} is actively stabilized to ± 1.5 ps, and the magnetic field is measured to 10^{-5} T, we estimate that this technique is capable of resolving spin lifetimes as long as 5 μs and $\Delta g/g \sim 0.1\%$. Furthermore, these parameters are easily measured for low magnetic fields, which is impractical in conventional spin beat [3] and Hanlé effect [11] measurements. Figure 3(d) shows the quality factor of the electron spins in the same sample, computed from the fits shown in Figs. 3(a)–3(b) according to the relation $Q = g\mu_B B T_2^*/h$. Also shown are data for a higher excitation density, which appears to follow the same trend but with a uniformly lower Q. We find three regimes: (a) a low-field region obeying a power law $Q \sim B^{0.8}$, (b) an intermediate regime where Q is independent of B, and (c) a high-field region in which Q decreases. Because dephasing of spin direction produces an effective lifetime which is inversely proportional to B, the resulting $Q \propto g/\Delta g$ is field independent. The plateau at $Q \sim 80$ seen in Fig. 3(d) suggests the possibility that spin dephasing limits the Q factors in this region, with a variation of $\Delta g/g = 0.28\%$. If one assumes that the electrons occupy an energy bandwidth kT, then the g-factor dispersion used above implies a limit to the Q factor of 88,

shown as a dotted line in Fig. 3(d). Given that the corresponding number of available states $D(E_F)kT$ exceeds the excitation density by more than ten, these data suggest we measure electrons with thermalized kinetic energies [14]. A temperature dependence within the intermediate field region is clearly desirable to test this hypothesis.

To probe electron-electron interactions within the low-field region, where spin dephasing does not contribute, we characterize the spin lifetime's power dependence. Optical pulse powers are converted to excitation densities N_{ex} using a focus spot area of $(50 \ \mu m)^2$ and a penetration depth of $\sim 8 \ \mu m$, obtained from absorption. The data [Fig. 4(a)] indicate a power law $T_2^* \sim N_{ex}^{-0.4}$, for $B = 0$, 0.2, and 6 T (not shown). Neither EY nor DP processes depend explicitly on the N_{ex} except through shifts in the average electron kinetic energy, which will be significant only when $N_{ex} \sim n$. Coulomb scattering between electrons can lead to substantial spin relaxation through the spin-orbit coupling in a manner similar to the EY mechanism, and a calculation for III-V semiconductors assuming classical statistics gives $T_{e-e} \sim N^{-1}(kT)^{-1/2}$, where N is the total electron density [15]. However, $N = n + N_{ex}$ in our case, which yields a rather weak dependence on N_{ex} until $N_{ex} \approx n$.

Temperature dependence often distinguishes between spin scattering processes [11,16]. For $n = 0$, 1×10^{18}, and 5×10^{18}, we measure T_2^* at 4 T and find only a weak temperature dependence from which we are unable to identify the operative relaxation mechanisms. For $n = 1 \times 10^{16}$, we see a much more dramatic temperature dependence, shown in Fig. 4(b) for $B = 0$ and 4 T. Below about 50 K, the spin lifetime becomes strongly field dependent, splitting into high- and low-field regimes. Dotted lines indicate EY and DP predictions for isotropic charged impurity scattering [17], where Γ_P is estimated from the measured mobility as $e/m^*\mu$, and contributions to the electron kinetic energy from doping have been included. The low-field behavior shows good agreement with DP above $T = 30$ K, below which a weaker temperature dependence $T_2^* \sim (kT)^{-1/2}$ is suggestive of electron-

electron scattering. Estimates taking $N = n + N_{ex}$, however, show that this mechanism is actually too strong and may require a more explicit consideration of doping effects [15]. These data support a transition to the EY mechanism below 30 K, accompanied by a strong field dependence which suppresses the high-field spin lifetimes.

In summary, studies of spin precession in n-type GaAs reveal that moderate doping yields significantly extended spin lifetimes. A new technique of resonant spin amplification provides detailed and valuable clues to the origin of spin relaxation in the regime of extremely long spin lifetimes, providing limits on the energy distribution of precessing spins and giving evidence of inhomogeneous broadening within a narrow window of magnetic fields. Spin amplification directly measures the strong field dependence of these long lifetimes which would otherwise be difficult to measure. If the applied field is well known, this technique also facilitates precise measurements of the electron g factor through shifts in the positions of the spin resonances. Conversely, if the g factor is well determined, the resonances may be used to pump the nuclear system through the Overhauser effect and to detect the coupling between electronic and nuclear spins.

[1] D. Divincenzo, Science **270**, 255 (1995); L. Sham, Science **277**, 1258 (1997).
[2] G. Prinz, Phys. Today **48**, 58 (1995).
[3] J.M. Kikkawa, I.P. Smorchkova, N. Samarth, and D.D. Awschalom, Science **277**, 1284 (1997).
[4] M. Oestreich *et al.*, Phys. Rev. B **53**, 7911 (1996).
[5] S.A. Crooker, D.D. Awschalom, J.J. Baumberg, F. Flack, and N. Samarth, Phys. Rev. B **56**, 7574 (1997).
[6] J. Shah, R.F. Leheny, and W. Wiegmann, Phys. Rev. B **16**, 1577 (1977).
[7] M.J. Yang *et al.*, Phys. Rev. B **47**, 6807 (1993).
[8] D. Pines and C. Slichter, Phys. Rev. **100**, 1014 (1955).
[9] R.J. Elliot, Phys. Rev. **96**, 266 (1954).
[10] M.I. D'Yakanov and V.I. Perel', Zh. Eksp. Teor. Fiz. **60**, 1954 (1971) [Sov. Phys. JETP **33**, 1053 (1971)].
[11] *Optical Orientation, Modern Problems in Condensed Matter Science,* edited by F. Meier and B.P. Zachachrenya (North-Holland, Amsterdam, 1984), Vol. 8.
[12] G. Bir, A. Aronov, and G. Pikus, Zh. Eksp. Teor. Fiz. **69**, 1382 (1975) [Sov. Phys. JETP **42**, 705 (1976)].
[13] A. Abragam, *The Principles of Nuclear Magnetism* (Clarendon, Oxford, 1961).
[14] The rapid energy relaxation of electrons in GaAs has been measured by A. Alexandrou, V. Berger, and D. Hulin, Phys. Rev. B **52**, 4654 (1995).
[15] P. Boguslawski, Solid State Commun. **33**, 389 (1980).
[16] K. Zerrouati *et al.*, Phys. Rev. B **37**, 1334 (1988); G. Fishman and G. Lampel, Phys. Rev. B **16**, 820 (1977).
[17] A.G. Aronov, G.E. Pikus, and A.N. Titkov, Zh. Eksp. Teor. Fiz. **84**, 1170 (1983) [Sov. Phys. JETP **57**, 680 (1983)].
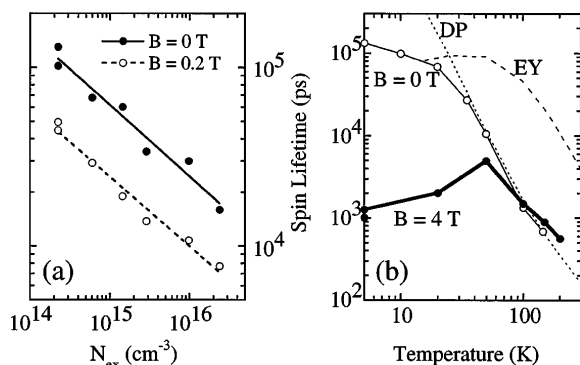

FIG. 4. (a) T_2^* vs N_{ex}. Solid lines are power-law fits to $T_2^* \sim N^{-0.4}$. Data are taken at 5 K. (b) T_2^* vs temperature for $n = 10^{16}$ at $B = 0$ and 4 T and $N_{ex} = 2 \times 10^{14}$ cm^{-3}. Dotted lines are DP and EY predictions.